Theor Chem Acc (2011) 130:687–700
DOI 10.1007/s00214-011-0983-z

REGULAR ARTICLE

On the dipolar electric field response of large systems

Michael Springborg · Bernard Kirtman

Received: 29 March 2011 / Accepted: 18 June 2011 / Published online: 9 July 2011

Abstract Whereas the definition of the dipole moment operator for any finite system, independent of its size, is trivial, it is only within the last 1–2 decades that expressions have been proposed (based on the independent particle approximation) for the equivalent operator of an infinite and periodic system. Using a quasi-one-dimensional system as an example, we show how different versions of these expressions can be derived and thereby formulate, for the first time, a multi-determinant treatment of the effect of electron correlation. Based on another version, an MP2 correlation treatment is suggested that relies entirely on already available procedures. In contrast with what is often assumed, we demonstrate that the so-called branch dependence of the dipole moment per unit of an infinite periodic system is directly related to bulk physical observables that depend on the terminations even for samples of a size that is well above the thermodynamic limit. In particular, the structural response to an electrostatic field is studied for a model system. It is shown how the effect of the terminations on the converse piezoelectric coefficient can be calculated and measured. In addition, we demonstrate the viability of the finite field nuclear relaxation treatment for determining the vibrational contribution to static (hyper)polarizabilities and dynamic non-linear optical processes in periodic systems.

Keywords Dipole moment · Polarizability · Chain compounds · Electrostatic fields

Dedicated to Professor Akira Imamura on the occasion of his 77th birthday and published as part of the Imamura Festschrift Issue.

M. Springborg (✉)
Physical and Theoretical Chemistry,
University of Saarland, Campus B2.2,
66123 Saarbrücken, Germany
e-mail: m.springborg@mx.uni-saarland.de

B. Kirtman
Department of Chemistry and Biochemistry,
University of California, Santa Barbara,
CA 93106, USA
e-mail: kirtman@chem.ucsb.edu

1 Introduction

All materials have finite spatial extensions. Nevertheless, it is often a good approximation to assume that they are infinite. The rationale behind this approximation is that the samples are sufficiently large so that (1) the thermodynamic limit is reached and (2) the effects due to the surfaces are negligible. If, in addition, the inner part of the system of interest consists of identical building blocks, so that deviations from regularity occur only at the surfaces, then the system can be treated as infinite and periodic. For the finite system containing N units, we may, in the thermodynamic limit, define the intensive property per unit that corresponds to the extensive property $\xi(N)$ as

$$\bar{\xi} = \lim_{N\to\infty} \frac{\xi(N)}{N} = \lim_{N\to\infty} \frac{1}{\Delta N}[\xi(N+\Delta N) - \xi(N)]. \quad (1)$$

$\bar{\xi}$ may be calculated from Eq. 1 or directly from results for the infinite, periodic system.

In the present contribution, we shall be interested in the case that ξ is the dipole moment. The reasons for studying the dipole moment are twofold. First, the response of any system to electric fields can be quantified through the dipole moment, which determines linear and

non-linear optical properties, as well as piezoelectricity, pyroelectricity, etc. Second, for the infinite periodic system, the theoretical/mathematical treatment of the dipole moment contains some special features that we want to relate to the physical properties of the very large, but finite, system.

For the sake of simplicity, the present paper will be restricted to quasi-one-dimensional systems. This is in tune with the pioneering work on such systems by Akira Imamura in whose honor we make this presentation. For quasi-one-dimensional systems, the surfaces of the system are the terminations.

The chains under consideration will be oriented along the z axis. From the standard definition of the dipole moment, i.e., being an integral over the total charge density times the position vector, the z component of the dipole moment of a long, but finite, chain can be split into a nuclear and an electronic part:

$$\mu_z = \int z\rho_{\text{tot}}(\mathbf{r})\mathrm{d}\mathbf{r} = \mu_n - \mu_e, \tag{2}$$

corresponding to the division of the total charge density as

$$\rho_{\text{tot}}(\mathbf{r}) = \rho_n(\mathbf{r}) + \rho_e(\mathbf{r}). \tag{3}$$

Within the Born–Oppenheimer approximation (which we will use), ρ_n will be a superposition of δ functions at the sites of the nuclei, whereas ρ_e will be determined quantum-mechanically either through a wavefunction-based (e.g., Hartree–Fock) or through a density-based (e.g., Kohn–Sham) approach. By calculating μ_z as a function of the number of units of the chain, $\mu_z(N)$, it is trivial to obtain $\bar{\mu}_z$. As we shall see, there will generally be a finite contribution from the surfaces independent of the size of the system.

Alternatively, one may attempt to calculate $\bar{\mu}_z$ directly from properties of the infinite, periodic system. Equation 2 suggests that such an approach may be non-trivial: the integrand is ill-behaved in the limit $z \to \pm\infty$ and it is also non-periodic. Indeed, it turns out that for the calculation of $\bar{\mu}_e$ one has to use a different approach as recognized, for example, by Blount [1] in the early 1960s. However, it was not until about twenty years ago that an intensive effort was initiated leading to several different procedures for calculating the dipole moment of an infinite periodic system, including both the permanent and induced contributions. Of these, the Berry phase treatment (also known as the modern theory of polarization; MTP) [2–6] and our own time-dependent vector potential approach (VPA) [7–16] have been the most fully developed. Despite their very different appearance, the MTP and the VPA are closely related. In fact, their equivalence in several aspects has now been shown (see for example, [12, 17]).

In this paper, we review some of the more recent developments with regard to the calculation of the dipolar electric field response of infinite periodic systems and the relationship between this response and that of a real finite macroscopic system. Both electronic and nuclear degrees of freedom will be considered as well as linear and non-linear properties. Our approach will be from a mixture of the MTP and VPA points of view. In addition, a number of new results will be mixed in with the review material.

In order to set the stage for making the connection between infinite periodic and finite macroscopic systems later on we begin, in the next section, with a brief treatment of $\bar{\mu}_z$ for large, but finite, chains. Although linear chains are used here and throughout, the principles developed are general and apply equally well to 2D and 3D systems. In Sect. 3, we turn to infinite periodic chains. The formal derivation of the single determinant MTP expression for the dipole moment given previously [10] is extended to include multi-determinant wavefunctions. In addition, wavefunction treatments of electron correlation within the framework of the VPA are discussed. Then in Sect. 4, we consider the electronic and nuclear response to an electrostatic field as determined by the dipole moment. The branch/phase dependence of the crystal orbitals in an infinite periodic treatment of a 1D chain is shown in Sect. 4 to be related to the effects caused by termination of that chain. This relationship is verified through model calculations based on the VPA Schrödinger-type self-consistent-field equation, which can also be derived from a version of the MTP treatment. Subsequently, in Sect. 5, we demonstrate how piezoelectric coefficients as well as vibrational non-linear optical properties—both static and dynamic—can be obtained from the nuclear response to a static field. Finally, our findings are discussed and summarized in Sect. 6.

For the sake of completeness, we mention here that, throughout this paper, we use atomic units so that, e.g., the magnitude of the elementary charge is set equal to unity, $|e| = 1$.

2 Long finite chain

A schematic representation of a long, but finite, 1D chain is shown in Fig. 1a. It is useful to split this system into three distinct spatial parts: a perfectly regular central region (C) where the electrons do not feel the finite size of the system, and two terminal regions (L and R). Using this spatial separation, the z component of the dipole moment is [13, 14]

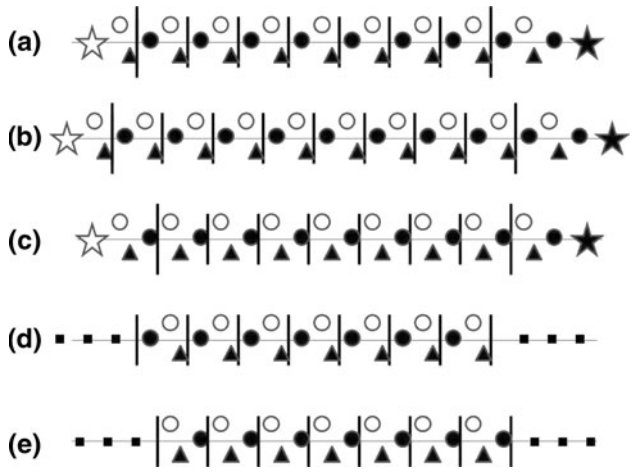

Fig. 1 Different schematic representations of long or infinite periodic chains. *Filled circles*, *empty circles*, and *filled triangles* represent three different types of atoms referred to in the text as *a*, *b*, and *c*, respectively. The *shorter vertical* lines separate different units. Cases (**a**), (**b**), and (**c**) correspond to finite chains; the *long vertical* lines separate *left* (L), *central* (C), and *right* (R) regions while the stars indicate the terminations. Cases (**a**) and (**b**) show the same chain but with two different lengths, whereas (**a**) and (**c**) differ in the way the units are defined. Cases (**d**) and (**e**) represent infinite, periodic chains that differ in the way the units are defined

$$\begin{aligned}\mu_z &= \int_L \rho(\mathbf{r})z\mathrm{d}\mathbf{r} + \int_C \rho(\mathbf{r})z\mathrm{d}\mathbf{r} + \int_R \rho(\mathbf{r})z\mathrm{d}\mathbf{r} \\ &= N_C\mu_C + \left[z_R\int_R \rho(\mathbf{r})\mathrm{d}\mathbf{r} + z_L\int_L \rho(\mathbf{r})\mathrm{d}\mathbf{r}\right] \\ &\quad + \left[\int_L \rho(\mathbf{r})(z-z_L)\mathrm{d}\mathbf{r} + \int_R \rho(\mathbf{r})(z-z_R)\mathrm{d}\mathbf{r}\right] \\ &= N_C\mu_C + (z_R - z_L)Q_R + \left[\int_L \rho(\mathbf{r})(z-z_L)\mathrm{d}\mathbf{r}\right. \\ &\quad \left. + \int_R \rho(\mathbf{r})(z-z_R)\mathrm{d}\mathbf{r}\right]. \end{aligned} \tag{4}$$

Here, μ_C is the z component of the dipole moment of a central unit, N_C is the number of units in C, and we will assume that the entire system is neutral so that the total charge in R, Q_R, is equal to $-Q_L$. Finally, z_R and z_L describe the centers of nuclear charge in the R and L regions, respectively. Per definition, the central units are neutral.

The spatial separation of the long finite chains in Fig. 1 is achieved when the length is such that there is a well-defined central region where the units are neutral and $\int_C \rho(\mathbf{r})z\mathrm{d}\mathbf{r}$ equals $N_C\ \mu_C$. We add that μ_C is not unique and that different definitions may lead to different values. Below we shall give one definition. According to our experience, it is not obvious at which size this thermodynamic limit is reached but, in general, more delocalized systems require greater chain lengths.

Increasing the length of the system by $\Delta N = 1$ unit (i.e., passing from Fig. 1a to Fig. 1b) increases N_C by 1 and $z_R - z_L$ by an amount equal to the lattice constant of the central region, a. From Eq. 1 we, then, obtain

$$\bar{\mu}_z = \mu_C + Q_R \cdot a. \tag{5}$$

Clearly, this result cannot depend on the original specification of the L, C, and R regions as long as C satisfies the separability conditions. Nonetheless, μ_C and the surface dipole can separately change as we now show by comparing Fig. 1a and Fig. 1c. In doing so, it will be assumed that the dipole moment can be calculated from atomic charges. This is illustrative, though not rigorous, because the electronic charge density cannot be strictly localized to the atomic centers. For Fig. 1a, we have

$$\mu_C = q_a z_a + q_b z_b + q_c z_c, \tag{6}$$

where q_i and z_i are the atomic charge and z position coordinate for the ith atom in one of the central units (see figure caption for identification of atoms a, b, and c). Passing to Fig. 1c, and keeping the origin (as defined by atomic positions) unchanged we see that z_b and z_c are unchanged whereas

$$\begin{aligned} z_a &\rightarrow z_a + a \\ Q_R &\rightarrow Q_R - q_a. \end{aligned} \tag{7}$$

Thus, the surface and unit cell contributions to the average dipole moment change by equal and opposite amounts. This means that the unit cell dipole moment by itself is not a physical property.

According to Eq. 5, the dipole moment per unit depends on the charge accumulated in the terminal regions which, at first glance, can vary widely. There are, however, restrictions on the surface charges as Vanderbilt and King-Smith [3] have shown. They write the electronic part of the dipole moment in terms of localized orbitals w_{lp}

$$\mu_e = \sum_l \sum_p \int |w_{lp}(\mathbf{r})|^2 z\mathrm{d}\mathbf{r}, \tag{8}$$

where w_{lp}, the pth orbital localized on the lth unit, is obtained by a unitary transformation of the occupied canonical orbitals. Then, using the idempotency of the density matrix, it is proved that the number of electrons associated with the terminal regions must be integral. This result has been coined 'charge quantization' [18] and implies that Q_R in Eq. 5 can only change by integers when introducing chemical modifications of the terminal regions (for instance by adding donor and acceptor groups).

In a naïve approach for an infinite periodic chain, one would assume that the dipole moment per unit is simply that of a single unit cell. Then, $\bar{\mu}_z$ would equal μ_C. From the discussion in this section, this would make $\bar{\mu}_z$ for an infinite periodic chain different from that of the long finite chain, since the contribution from the charge at the terminations is removed. Moreover, the dipole moment per unit would depend on the choice of the unit cell as is evident from Fig. 1d, e. Although this treatment is sometimes used (for a more detailed discussion, see e.g., [19–21]), it is not correct as we show in the next section.

3 Infinite periodic chain

For a finite system with N electrons, the (origin-dependent) electronic part of the dipole moment is defined as

$$\mu_e = \left\langle \Psi \left| \sum_{i=1}^{N} z_i \right| \Psi \right\rangle, \tag{9}$$

where Ψ is the N-electron wavefunction. When the system is treated as infinite and periodic, a different approach must be used. For that case, the single-particle crystal orbitals may be written as Bloch waves,

$$\psi_j(k, \mathbf{r}) = \mathrm{e}^{ikz} u_j(k, \mathbf{r}). \tag{10}$$

In a practical calculation, the infinite number of k points is replaced by a finite set of K equidistant points that sample the 1st Brillouin zone which corresponds to the interval $]-\frac{\pi}{a};\frac{\pi}{a}]$. This gives a k spacing of

$$\Delta k = \frac{2\pi}{Ka}, \tag{11}$$

where a is the unit cell length. We emphasize that the K unit cells form a Born von Kármán zone and it is assumed that every quantity has the periodicity of this zone. Given a single determinant wavefunction composed of crystal orbitals, the problem is to identify an operator whose expectation value will yield the dipole moment per unit cell.

3.1 MTP expressions for independent particles

First, we consider the case $N = 1$. In that instance, we seek a one-electron operator $\hat{A}$ that satisfies the following:

- The expectation value for the ground state can be calculated as (cf. Eq. 9):

$$\langle\psi|\hat{A}|\psi\rangle = \langle\psi|f(z)|\psi\rangle, \tag{12}$$

where $f(z)$ possesses the periodicity of the Born von Kármán zone.

- In the limit $K \to \infty$ or, equivalently, $\Delta k \to 0$

$$f(z) = a_0 + a_1 z + a_2 z^2 + \cdots \simeq a_0 + a_1 z, \tag{13}$$

so that the expectation value of Eq. 12 becomes

$$\langle\psi|\hat{A}|\psi\rangle = \langle\psi|f(z)|\psi\rangle \simeq f(\langle\psi|z|\psi\rangle), \tag{14}$$

or, by inverting Eq. 14,

$$\langle\psi|z|\psi\rangle = f^{-1}(\langle\psi|\hat{A}|\psi\rangle). \tag{15}$$

An operator that satisfies the above criteria has been presented by Blount [1] and will be used here. Given that an arbitrary $\psi(\mathbf{r})$ can be expanded in terms of Bloch waves as

$$\psi(\mathbf{r}) = \sum_k \sum_j \psi_j(k, \mathbf{r}) f_j(k) = \sum_k \sum_j \mathrm{e}^{ikz} u_j(k, \mathbf{r}) f_j(k), \tag{16}$$

then, as Blount proposed, one may write

$$\begin{aligned} \hat{z}\psi(\mathbf{r}) &= (i\hat{D}'' - i\hat{D}')\psi(\mathbf{r}) \\ &\equiv \sum_k \sum_j \left\{ i\mathrm{e}^{ikz} \frac{\partial}{\partial k} \mathrm{e}^{-ikz} \left[f_j(k)\psi_j(k, \mathbf{r}) \right] \right. \\ &\quad \left. -i \frac{\partial}{\partial k} \left[f_j(k)\psi_j(k, \mathbf{r}) \right] \right\}. \end{aligned} \tag{17}$$

That is to say, we may take the desired operator to be $\hat{A} = i(\hat{D}'' - \hat{D}')$.

As mentioned above, in a practical calculation, only a finite set of equidistant k points is used, or, equivalently, $\hat{A}$ has to have the periodicity of the Born von Kármán zone. Therefore, the derivatives of any function $g(k)$ with respect to k have to be replaced by finite-difference approximations. Here, we consider three different possibilities,

$$\begin{aligned} g'(k) \simeq g'_+(k) &= \frac{g(k + \Delta k) - g(k)}{\Delta k} \\ g'(k) \simeq g'_-(k) &= \frac{g(k) - g(k - \Delta k)}{\Delta k} \\ g'(k) \simeq g'_0(k) &= \frac{g(k + \Delta k) - g(k - \Delta k)}{2\Delta k}. \end{aligned} \tag{18}$$

The middle line of Eq. 18, for example, leads to the finite-difference approximations for $\hat{D}'$ and $\hat{D}''$:

$$\begin{aligned} \hat{\Delta}'_-\psi(\mathbf{r}) &= \frac{1}{\Delta k} \sum_k \sum_j \left[\psi_j(k, \mathbf{r}) f_j(k) \right. \\ &\quad \left. -\psi_j(k - \Delta k, \mathbf{r}) f_j(k - \Delta k) \right] \\ \hat{\Delta}''_-\psi(\mathbf{r}) &= \frac{1}{\Delta k} \sum_k \sum_j \mathrm{e}^{ikz} \left[u_j(k, \mathbf{r}) f_j(k) \right. \\ &\quad \left. -u_j(k - \Delta k, \mathbf{r}) f_j(k - \Delta k) \right]. \end{aligned} \tag{19}$$

For $\hat{\Delta}'_+$ and $\hat{\Delta}''_+$, the corresponding expressions are the same except that, within the square brackets, k is replaced by

$k + \Delta k$. For the third possibility in Eq. 18, we simply use the average of the + and − formulas. It is, then, fairly straightforward to obtain the corresponding three expressions for the matrix element of Eq. 12,

$$\begin{aligned}
\langle\psi|(-i\hat{\Delta}'_- + i\hat{\Delta}''_-)|\psi\rangle &= \left\langle \psi \middle| \frac{i}{\Delta k}(1 - e^{i\Delta k z}) \middle| \psi \right\rangle \\
&= \frac{i}{\Delta k}(1 - S^+) \\
\langle\psi|(-i\hat{\Delta}'_+ + i\hat{\Delta}''_+)|\psi\rangle &= \left\langle \psi \middle| \frac{i}{\Delta k}(e^{-i\Delta k z} - 1) \middle| \psi \right\rangle \\
&= \frac{i}{\Delta k}(S^- - 1) \\
\langle\psi|(-i\hat{\Delta}'_0 + i\hat{\Delta}''_0)|\psi\rangle &= \left\langle \psi \middle| \frac{\sin(\Delta k z)}{\Delta k} \middle| \psi \right\rangle \\
&= \frac{1}{2i\Delta k}(S^+ - S^-),
\end{aligned} \tag{20}$$

where we have introduced

$$S^{\pm} = \langle\psi|e^{\pm i\Delta k z}|\psi\rangle. \tag{21}$$

Finally, the approximation of Eq. 14 gives

$$\begin{aligned}
\langle\psi|z|\psi\rangle &\simeq \frac{-i}{\Delta k}\ln S^+ \simeq \frac{1}{\Delta k}\mathrm{Im}\ln S^+ \\
\langle\psi|z|\psi\rangle &\simeq \frac{i}{\Delta k}\ln S^- \simeq \frac{-1}{\Delta k}\mathrm{Im}\ln S^- \\
\langle\psi|z|\psi\rangle &\simeq \frac{1}{\Delta k}\mathrm{Arcsin}\left[\frac{1}{2i}(S^+ - S^-)\right].
\end{aligned} \tag{22}$$

Next, we turn to the many-electron case using the single determinant wavefunction

$$\Psi_{\mathbf{i}}(\mathbf{r}) = \frac{1}{\sqrt{N!}}\hat{\mathcal{A}}\left[\psi_{i_1}(\mathbf{r}_1)\psi_{i_2}(\mathbf{r}_2)\cdots\psi_{i_N}(\mathbf{r}_N)\right] \tag{23}$$

in which $\mathbf{r} = (\mathbf{r}_1, \mathbf{r}_2, \ldots, \mathbf{r}_N)$, $\hat{\mathcal{A}}$ is the antisymmetrizer, and N is the number of electrons in the Born von Kármán zone. If each single-particle wavefunction is expanded in Bloch functions as in Eq. 16, then the expression for the operator

$$\hat{Z} = \sum_{i=1}^{N} \hat{z}_i \tag{24}$$

acting on $\Psi_{\mathbf{i}}(\mathbf{r})$ becomes

$$\begin{aligned}
\hat{Z}\Psi_{\mathbf{i}}(\mathbf{r}) = i\exp\left(i\sum_{n=1}^{N} k_n z_n\right)\left(\sum_{n=1}^{N}\frac{\partial}{\partial k_n}\right) \\
\times\left[\exp\left(-i\sum_{n=1}^{N} k_n z_n\right)\Psi_{\mathbf{i}}(\mathbf{r})\right] \\
- i\left(\sum_{n=1}^{N}\frac{\partial}{\partial k_n}\right)\Psi_{\mathbf{i}}(\mathbf{r}).
\end{aligned} \tag{25}$$

As in the single-electron case, we replace the k-derivatives with finite-difference approximations and, after some tedious but trivial manipulations, end up with expressions that have the same form as in Eq. 20 except that Z replaces z and $\det\underline{\underline{S}}^{\pm}$ replaces $S^{\pm}$. For example, the first line of Eq. 20 becomes:

$$\begin{aligned}
&\langle\Psi_{\mathbf{i}}(\mathbf{r})|(-i\hat{\Delta}'_- + i\hat{\Delta}''_-)|\Psi_{\mathbf{i}}(\mathbf{r})\rangle \\
&\quad= \left\langle \Psi_{\mathbf{i}}(\mathbf{r}) \middle| \frac{i}{\Delta k}\left(1 - e^{i\Delta\mathbf{k}\cdot\mathbf{z}}\right) \middle| \Psi_{\mathbf{i}}(\mathbf{r}) \right\rangle \\
&\quad= \frac{i}{\Delta k}\left(1 - \det\underline{\underline{S}}^+\right).
\end{aligned} \tag{26}$$

Here

$$\left(\underline{\underline{S}}^{\pm}\right)_{lm} = \langle\psi_l(\mathbf{r})|e^{\pm i\Delta k z}|\psi_m(\mathbf{r})\rangle. \tag{27}$$

Then, using the analog of Eq. 14 the dipole moment per unit,

$$\bar{\mu} = \frac{1}{K}\langle\Psi_{\mathbf{i}}|z_1 + z_2 + \cdots + z_N|\Psi_{\mathbf{i}}\rangle, \tag{28}$$

becomes

$$\bar{\mu}_{\mathrm{R}} = \frac{a}{2\pi}\mathrm{Im}\ln\det\underline{\underline{S}}^+ = -\frac{a}{2\pi}\mathrm{Im}\ln\det\underline{\underline{S}}^- \tag{29}$$

which is the expression that Resta has suggested within the MTP [4]. Alternatively, one may also consider

$$\bar{\mu}_0 = \frac{a}{2\pi}\mathrm{Arcsin}\left[\frac{1}{2i}\left(\det\underline{\underline{S}}^+ - \det\underline{\underline{S}}^-\right)\right]. \tag{30}$$

Our numerical calculations [10] have shown, however, that the latter expression converges slower as a function of K than is the case for $\bar{\mu}_{\mathrm{R}}$.

When Bloch waves, Eq. 10, are used as the single-particle eigenfunctions the $\underline{\underline{S}}^{\pm}$ matrices have a particularly simple structure (see Fig. 2),

$$\begin{aligned}
\left[S_{j_1 j_2}(k_1, k_2)\right]^{\pm} &= \langle\psi_{j_1}(k_1, \mathbf{r})|e^{\pm i\Delta k z}|\psi_{j_2}(k_2, \mathbf{r})\rangle \\
&= \delta_{k_1, k_2 \pm \Delta k}\langle u_{j_1}(k_1, \mathbf{r})|u_{j_2}(k_2, \mathbf{r})\rangle.
\end{aligned} \tag{31}$$

Obviously, the $\underline{\underline{S}}^{\pm}$ matrices, which determine the dipole moment per unit, are not diagonal in k.

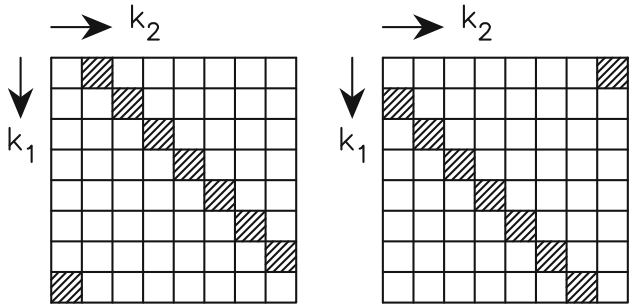

Fig. 2 The structure of the $\underline{\underline{S}}^{\pm}$ matrices in a Bloch-function representation

In order to proceed further, we use the first-order Taylor series expansion

$$u_j(k \pm \Delta k, \mathbf{r}) \simeq u_j(k, \mathbf{r}) \pm \Delta k \frac{\partial}{\partial k} u_j(k, \mathbf{r}), \tag{32}$$

which gives

$$\begin{aligned} &\langle \psi_{j_1}(k, \mathbf{r}) | \mathrm{e}^{\pm i \Delta k z} | \psi_{j_2}(k \mp \Delta k, \mathbf{r}) \rangle \\ &\quad \simeq \delta_{j_1 j_2} \mp \Delta k \left\langle u_{j_1}(k, \mathbf{r}) \left| \frac{\partial}{\partial k} \right| u_{j_2}(k, \mathbf{r}) \right\rangle \end{aligned} \tag{33}$$

so that, to lowest order in Δk,

$$\begin{aligned} \ln \det \underline{\underline{S}}^{\pm} &= \ln \left[\prod_k \prod_j \left(1 \mp \Delta k \left\langle u_j(k, \mathbf{r}) \left| \frac{\partial}{\partial k} \right| u_j(k, \mathbf{r}) \right\rangle \right) \right] \\ &\simeq \ln \left[1 \mp \Delta k \sum_k \sum_j \left\langle u_j(k, \mathbf{r}) \left| \frac{\partial}{\partial k} \right| u_j(k, \mathbf{r}) \right\rangle \right] \\ &\simeq \mp \Delta k \sum_k \sum_j \left\langle u_j(k, \mathbf{r}) \left| \frac{\partial}{\partial k} \right| u_j(k, \mathbf{r}) \right\rangle. \end{aligned} \tag{34}$$

Then

$$\begin{aligned} \bar{\mu}_{\mathrm{R}} &= \frac{a}{2\pi} \mathrm{Im} \ln \det \underline{\underline{S}}^{+} = -\frac{a}{2\pi} \mathrm{Im} \ln \det \underline{\underline{S}}^{-} \\ &\simeq \frac{a}{2\pi} \mathrm{Im} \left[\Delta k \sum_k \sum_j \left\langle u_j(k, \mathbf{r}) \left| \frac{\partial}{\partial k} \right| u_j(k, \mathbf{r}) \right\rangle \right] \\ &= \frac{i}{K} \sum_k \sum_j \left\langle u_j(k, \mathbf{r}) \left| \frac{\partial}{\partial k} \right| u_j(k, \mathbf{r}) \right\rangle \equiv \bar{\mu}_{\mathrm{KSV}}. \end{aligned} \tag{35}$$

The last expression is the one that was proposed by King-Smith and Vanderbilt within the MTP [2].

Within an LCAO approach, the single-particle wavefunctions are expanded in terms of Bloch waves formed from atom-centered basis functions, i.e.,

$$\psi_j(k, \mathbf{r}) = \sum_p C_{pj}(k) \chi_p(k, \mathbf{r}) \tag{36}$$

where

$$\chi_p(k, \mathbf{r}) = \frac{1}{\sqrt{K}} \sum_m \mathrm{e}^{ikam} \chi_{pm}(\mathbf{r}), \tag{37}$$

and χ_{pm} is the pth basis function of the mth unit. Then

$$\begin{aligned} \bar{\mu}_e &= \frac{i}{K} \sum_j \sum_k \left\langle u_j(k, \mathbf{r}) | \frac{\partial}{\partial k} u_j(k, \mathbf{r}) \right\rangle \\ &= \frac{1}{K} \sum_j \sum_m \sum_k \mathrm{e}^{ikma} \sum_{pq} C^*_{qj}(k) \langle \chi_{q0} | z - ma | \chi_{pm} \rangle C_{pj}(k) \\ &\quad + \frac{i}{K} \sum_j \sum_m \sum_k \mathrm{e}^{ikma} \sum_{pq} C^*_{qj}(k) \langle \chi_{q0} | \chi_{pm} \rangle \frac{\mathrm{d}}{\mathrm{d}k} C_{pj}(k) \\ &\equiv \bar{\mu}_{e,\mathrm{charge}} + \bar{\mu}_{e,\mathrm{current}}, \end{aligned} \tag{38}$$

whereby $\bar{\mu}_e$ is split into so-called charge and current contributions. The former is the expectation value for a function that resembles z but is piecewise linear with the periodicity of the lattice. The two term expression in Eq. 38 is the one that is used in the VPA, although it is derived in a more succinct manner. Finally, we may add the nuclear contribution, which modifies only the charge term, to obtain

$$\bar{\mu} = \bar{\mu}_{\mathrm{charge}} + \bar{\mu}_{\mathrm{current}}. \tag{39}$$

As mentioned at the beginning of Sect. 2, the dipole moment of one unit of the central region of a long, but finite chain, μ_C, is not unique. One possibility is to identify it with the $\bar{\mu}_{\mathrm{charge}}$, obtained using a basis set for which $\langle \chi_{p_1} | z | \chi_{p_2} \rangle$ vanishes when $p_1 \neq p_2$. This corresponds to calculating μ_C with the functions of only one unit cell. By comparing with Eq. 5 one, then obtains

$$\begin{aligned} \mu_C &= \bar{\mu}_{\mathrm{charge}} \\ Q_R \cdot a &= \bar{\mu}_{\mathrm{current}}. \end{aligned} \tag{40}$$

By construction, the first identity holds, whereby the second identity must hold. Numerical studies confirm these relations.

3.2 Wavefunction treatment of electron correlation

Electron correlation can, of course, be incorporated within a single-particle formulation by means of density functional theory. On the other hand, from the wavefunction point of view, we can also readily extend the MTP treatment given above to include configuration interaction. A multi-determinant wavefunction can be written in the form

$$\Psi(\mathbf{r}) = \sum_{\mathbf{i}} C_{\mathbf{i}} \Psi_{\mathbf{i}}(\mathbf{r}), \tag{41}$$

where the individual Slater determinants are given in Eq. 23. It is, then, straightforward to generalize Eq. 26. The first line, for example, simply becomes

$$\begin{aligned} &\left\langle \Psi(\mathbf{r}) \left| (-i\hat{\Delta}'_- + i\hat{\Delta}''_-) \right| \Psi(\mathbf{r}) \right\rangle \\ &\quad = \left\langle \sum_{\mathbf{i}} C_{\mathbf{i}} \Psi_{\mathbf{i}}(\mathbf{r}) \left| \frac{i}{\Delta k} \left(1 - \mathrm{e}^{i \Delta \mathbf{k} \cdot \mathbf{z}} \right) \right| \sum_{\mathbf{i}} C_{\mathbf{i}} \Psi_{\mathbf{i}}(\mathbf{r}) \right\rangle. \end{aligned} \tag{42}$$

Using arguments similar to those in the previous subsection, we define

$$\langle \Psi_{\mathbf{i}}(\mathbf{r}) | \mathrm{e}^{\pm i \Delta \mathbf{k} \cdot \mathbf{z}} | \Psi_{\mathbf{j}}(\mathbf{r}) \rangle = \det \underline{\underline{S}}^{\pm}_{\mathbf{i},\mathbf{j}} \tag{43}$$

with

$$\left(\underline{\underline{S}}^{\pm}_{\mathbf{i},\mathbf{j}} \right)_{lm} = \langle \psi_{i_l}(\mathbf{r}) | \mathrm{e}^{\pm i \Delta k z} | \psi_{j_m}(\mathbf{r}) \rangle. \tag{44}$$

Here, ψ_{i_l} is the lth spin-orbital of the $\mathbf{i}$th Slater determinant. Thus, Eq. 42 can be written as

$$\begin{aligned}&\langle\Psi(\mathbf{r})|(-i\hat{\Delta}'_{-}+i\hat{\Delta}''_{-})|\Psi(\mathbf{r})\rangle\\&\quad=\left\langle\Psi(\mathbf{r})\left|\frac{i}{\Delta k}\left(1-\mathrm{e}^{i\Delta\mathbf{k}\cdot\mathbf{z}}\right)\right|\Psi(\mathbf{r})\right\rangle\\&\quad=\frac{i}{\Delta k}\left\{1-\sum_{\mathbf{i},\mathbf{j}}C^{*}_{\mathbf{i}}C_{\mathbf{j}}\left[\det\underline{\underline{S}}^{+}_{\mathbf{i},\mathbf{j}}\right]\right\}.\end{aligned}\tag{45}$$

This is the generalization of the single determinant case (cf. Eq. 26). Using an approximation analogous to that of Eq. 14, we arrive at the generalization of Eq. 29,

$$\begin{aligned}\bar{\mu}_{\mathrm{R}}&=\frac{a}{2\pi}\,\mathrm{Im}\ln\left\{\sum_{\mathbf{i},\mathbf{j}}C^{*}_{\mathbf{i}}C_{\mathbf{j}}\left[\det\underline{\underline{S}}^{+}_{\mathbf{i},\mathbf{j}}\right]\right\}\\&=-\frac{a}{2\pi}\,\mathrm{Im}\ln\left\{\sum_{\mathbf{i},\mathbf{j}}C^{*}_{\mathbf{i}}C_{\mathbf{j}}\left[\det\underline{\underline{S}}^{-}_{\mathbf{i},\mathbf{j}}\right]\right\}.\end{aligned}\tag{46}$$

Finally, by applying a Taylor expansion as in Eq. 32, and keeping only the terms to lowest order in Δk, we obtain after some manipulation

$$\begin{aligned}\bar{\mu}_{\mathrm{KSV}}=\frac{i}{K}\Bigg[&\sum_{\mathbf{i}}C^{*}_{\mathbf{i}}C_{\mathbf{i}}\sum_{k}\sum_{j}\left\langle u_{i_j}(k,\mathbf{r})\left|\frac{\partial}{\partial k}\right|u_{i_j}(k,\mathbf{r})\right\rangle\\&+\sum_{\mathbf{i},\mathbf{j}}{}'C^{*}_{\mathbf{i}}C_{\mathbf{j}}\left\langle u_{i_0}(k,\mathbf{r})\left|\frac{\partial}{\partial k}\right|u_{j_0}(k,\mathbf{r})\right\rangle\Bigg].\end{aligned}\tag{47}$$

In the second summation of Eq. 47, only Slater determinants differing in exactly one spin-orbital (as specified by i_0 and j_0) are included.

One could develop a corresponding time-dependent configuration interaction treatment within the VPA. However, the most obvious way to approach the electron correlation problem using wavefunctions is by means of the time-dependent many-body perturbation theory/coupled cluster approach. In principle, the time-dependent Møller–Plesset second-order perturbation treatment (TD-MP2) of Hattig and Hess [22] may be utilized, for example, together with local-MP2 for periodic systems [23]. Both procedures have been separately implemented and their combination should be reasonably straightforward. Thinking further ahead one could go on to consider the CC2 method as well as coupled cluster doubles (CCD) and/or singles and doubles (CCSD).

4 Branch dependence and structural response to an electrostatic field

Using the $\bar{\mu}_{\mathrm{KSV}}$ expression for the dipole moment and the fact that the unit cells of the infinite, periodic system are neutral, it can be demonstrated that two different choices of the unit cell, like those of Fig. 1d, e, cannot change the dipole moment per unit. Since the unit cells are neutral, this finding is independent of the choice of the origin (provided, again, it is defined with respect to atomic positions) in the two cases. On the other hand, the assumption above that the two different choices lead to identical single-particle orbitals (including band- and k-dependent phase factors), may or may not be fulfilled. For reasons to be discussed in the paragraphs immediately below, we may, in fact, obtain two different values for the electronic part of the dipole moment per unit. These values can, however, differ only by a lattice vector.

As implied above, there is an ambiguity in the value of $\bar{\mu}_{\mathrm{R}}$ calculated from Eq. 29. According to this expression, the dipole moment per unit is written as a constant times the imaginary part of the natural logarithm of a complex number. Writing the complex number as an amplitude times a phase factor, the imaginary part of the natural logarithm is simply the phase. The phase, however, is given only up to an integer times 2π, whereby the dipole moment per unit contains an unknown integral multiple of the lattice constant, $\tilde{n}\cdot a$. In the VPA, this phase is related to the phases of the crystal orbitals. Values of $\bar{\mu}_z$ that differ by $\tilde{n}\cdot a$ are said to belong to different branches, and it is often assumed to be impossible to fix the branch uniquely (i.e., to identify the 'missing integer' $\tilde{n}$). In that event, one can only determine changes in $\bar{\mu}_z$ under some process during which it is assumed that the branch does not change (see e.g., [6]).

On the other hand, any finite system, no matter how large it may be, will have a unique value of $\bar{\mu}_z$ as shown in Sect. 2. Modifying such a system through terminal substitutions may change the charge at the terminations and thereby $\bar{\mu}_z$. However, the former can change only by an integral number of electrons and the latter only by the same integer times the lattice constant. The question that naturally arises, then, is whether there is a connection between the missing integer associated with different branches in periodic calculations and the integer associated with the surface charge in calculations on long finite chains. This can be studied by monitoring the structural response (and related properties) to an applied electrostatic field. That is to say, the effect on the structure obtained with different chain terminations can be compared with periodic chain results for which the missing integer is given different values.

4.1 Formalism

For the purpose of checking formalism and computational approaches, models can provide excellent test systems. They are especially useful in this case because of the need for comparison of the infinite periodic system with corresponding large finite systems. The latter have to be large

enough that a central region can be defined. Furthermore, model studies may provide useful, general understanding. In that spirit, we present a new study, based on our previous model that not only corroborates our earlier results [15] but allows us, in Sect. 5, to demonstrate the feasibility of determining properties not previously obtained for a nanomaterial.

We begin with a discussion of the formal theory. For any finite system, describing the interaction with an electrostatic field by means of the scalar potential, changes the Hamiltonian operator according to

$$\hat{H} \rightarrow \hat{H} - \mu_z E, \tag{48}$$

where we have assumed that the field E is along the chain (z) axis. Upon inclusion of the electrostatic field, the single-particle [Hartree–Fock (HF) or Kohn–Sham (KS)] equation contains an extra electronic term, $-z\ E$, that is easily treated (at a given geometry the nuclear term is simply an additive constant). Of course, in doing so, one must take into account the fact that the Hamiltonian is a function of the density matrix (or density) which, in turn, depends upon the field.

The situation is different for the infinite, periodic system. Within the single-particle formulation, the operator for the dipole moment per unit is one of several choices determined by the several choices for the expectation value that we gave in Sect. 3.1. It turns out to be most convenient to use $\bar{\mu}_{\mathrm{KSV}}$ of Eq. 35. In fact, this same expression is exactly the one that appears in the basic Schrödinger-like VPA equation [8, 9], i.e.,

$$\sum_p \left\{ F_{qp}(k) - E\left[M_{qp}(k) + iS_{qp}(k)\frac{\partial}{\partial k}\right]\right\} C_{jp}(k) = \epsilon_j(k) \sum_p S_{qp}(k) C_{jp}(k), \tag{49}$$

where

$$\begin{aligned} S_{qp}(k) &= \sum_l \mathrm{e}^{ikal}\langle \chi_{q0}|\chi_{pl}\rangle \\ F_{qp}(k) &= \sum_l \mathrm{e}^{ikal}\langle \chi_{q0}|\hat{F}|\chi_{pl}\rangle \\ M_{qp}(k) &= \sum_l \mathrm{e}^{ikal}\langle \chi_{q0}|z - la|\chi_{pl}\rangle = \sum_l \mathrm{e}^{-ikal}\langle \chi_{ql}|z|\chi_{p0}\rangle \end{aligned} \tag{50}$$

are the overlap matrix, the Fock (or analogous Kohn–Sham) matrix, and the sawtooth (or charge) contribution to the dipole matrix, respectively. Of course, the Fock matrix depends implicitly on E through the density and/or density matrix.

Solving Eq. 49, particularly for a finite field, is non-trivial. It is not a standard eigenvalue problem due to the presence of the derivative with respect to k. Moreover, since the expansion coefficients $C_{jp}(k)$ may contain k and j (=band-) dependent phase factors that are essentially random, their derivatives with respect to k are numerically ill-behaved. In order to solve these problems, we have developed an efficient and numerically stable phase-smoothing procedure whose details will not be discussed here [12]. We have also demonstrated how the optimized field-dependent structure can be calculated using analytical derivatives [12]. These analytical derivatives were used in the calculations to be reported below.

4.2 Model

Our model is a linear chain with alternating atoms (denoted A and B) and alternating bond lengths. For the infinite, periodic system, the structure is described through the lattice constant, a, and a parameter u_0 that quantifies the alternating bond lengths $a/2 - 2u_0$ and $a/2 + 2u_0$. For the infinite periodic chain in the absence of the electrostatic field, the two structures differing in the sign of u_0 are energetically degenerate. We shall here study only the case that $u_0 > 0$. This corresponds to choosing the unit cell so that the shorter interatomic bonds are between atoms of the same unit cell and the longer ones are between atoms of neighboring unit cells.

There are 4 electrons per repeat unit and nuclear charges of $2|e|$ on each atom. We use an HF-like approximation with a basis set that consists of a pair of orthonormal functions centered on each atom. In order to calculate various matrix elements analytically, the mathematical expressions for one of the two basis functions at the atom X (placed at z_0) is defined as $\chi_{\mathrm{X},1}(z) = \frac{1}{\sqrt{w_{\mathrm{X},1}}}$ for $|z - z_0| \leq \frac{w_{\mathrm{X},1}}{2}$, and zero elsewhere; the other function is defined as $\chi_{\mathrm{X},2}(z) = \frac{1}{\sqrt{w_{\mathrm{X},2}}}$ for $\frac{w_{\mathrm{X},2}}{4} \leq |z - z_0| \leq \frac{w_{\mathrm{X},2}}{2}, \frac{-1}{\sqrt{w_{\mathrm{X},2}}}$ for $|z - z_0| \leq \frac{w_{\mathrm{X},2}}{4}$, and zero elsewhere. The widths, w (obeying $w_{\mathrm{X},\,1} > w_{\mathrm{X},\,2}$), were kept sufficiently small so that functions on non-neighboring atoms do not overlap.

We write the field-free N-electron Hamiltonian as a sum of one- and two-electron operators,

$$\hat{H} = \sum_{n=1}^{N} \hat{h}_0(n) + \frac{1}{2} \sum_{n_1 \neq n_2 = 1}^{N} \hat{v}(n_1, n_2). \tag{51}$$

The one-electron matrix element $\langle \chi_{qm}|\hat{h}_0|\chi_{pl}\rangle$ is assumed to be non-zero only for $(q, m) = (p, l)$ (in which case it is a constant that depends only on the type of atom and on the basis function) and for the two atoms at which the two basis functions are centered being nearest neighbors (in which case it depends linearly on the interatomic distance). Here, the second index (i.e. l or m) refers to the unit cell and the first index refers to the basis function. Of the two-electron matrix elements, only $\langle \chi_{ql}\chi_{ql}|\hat{v}|\chi_{ql}\chi_{ql}\rangle$ is assumed

to be non-zero. Moreover, $\langle \chi_{qm}|z|\chi_{pl}\rangle = \delta_{m,l}\delta_{q,p}z_{qm}$, where z_{qm} is the z coordinate of the atom where the function is centered. Finally, for the purpose of having a pre-chosen minimum energy structure in the field-free case, we include an elastic term in the potential for nuclear motion, which contains 2nd and 4th order terms in nearest- and next-nearest-neighbor changes in the interatomic distance.

In total, our model is very similar to a standard semi-empirical electronic structure method, except that we do not attempt to interpret the results as being those of specific systems. In an earlier work [15], we used this model for both long finite chains and infinite periodic systems. We were thereby able to demonstrate that the 'missing integer', or branch, in the infinite chain calculations exactly replicated the effect of charge localization in the terminal regions of the corresponding finite system. Although the parameters here are somewhat different (see below), the results corroborate our previous finding.

4.3 Structural response to electrostatic field for model systems

Since the relationship between the missing integer/branch for the infinite periodic system and the terminal charges of the corresponding finite system is well established, it is useful here to concentrate on the former: the reason is simply that the calculations are many orders of magnitude faster for the infinite periodic system. In Fig. 3, we show the variation in the structure as a function of the external electrostatic field. Three different sets of results are displayed; they have been obtained by choosing three different values of the missing integer, $\tilde{n}$. Given the relationship between $\tilde{n}$ and the terminal charges of the long finite chain, one of the three different cases corresponds to having a total charge at the terminations equal to $\pm Q$, which is the smallest possible value. For the two other cases, Q is changed from that value by ± 2. Figure 3 demonstrates accordingly that the field-dependent structure for the central region of the finite chain depends on the terminations. In particular, the converse piezoelectric effect, which describes how the spatial extension of the macroscopic material varies with the field, clearly depends on the terminations. The dependence of the structural response to the electric field on $\tilde{n}$ depends on the elastic properties of the system. Our calculations were performed on a model with parameters that yield a significant, though not dramatic, dependence on $\tilde{n}$. By varying parameter values, both much stronger and much weaker dependencies can be obtained.

Further information on the properties of the system at hand can be found in Fig. 4. The number of electrons on the A atom, N_A, depends only weakly on E when the structure is not relaxed (top left hand panel; note vertical

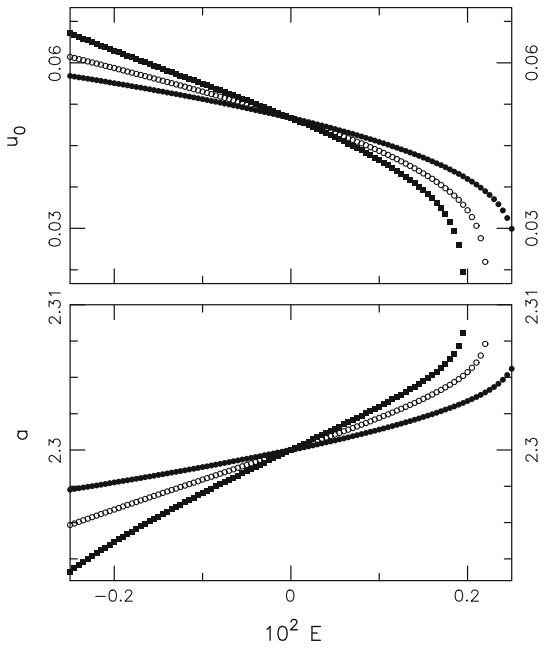

Fig. 3 Optimized values of the lattice constant (*lower* part), a, and bond-length alternation parameter (*upper* part), u_0, for the infinite periodic chain as a function of the field, E. The *different symbols* mark results for different values of the missing integer, $\tilde{n}$.

scale). Moreover, in the same panel, we find that N_A is independent of $\tilde{n}$. The situation changes when the structure is allowed to relax (top right hand panel). Then, there is a much stronger dependence of N_A on E, and, most importantly, N_A depends on $\tilde{n}$. It turns out that the latter effect is solely due to the dependence of the lattice constant a on $\tilde{n}$: keeping a fixed removes the dependence of all properties on $\tilde{n}$.

As also seen in Fig. 4, similar results are found for $\bar{\mu}$. In order to improve the comparison between the results for different values of $\tilde{n}$, we have modified the dipole moment per unit (as well as the contribution due to the current term to be discussed below) for a given $\tilde{n}$ by an integer times the field-free lattice constant. Note that for a given $\tilde{n}$, $\bar{\mu}$ depends much more strongly on E when the structure is allowed to relax than it does without relaxation.

Finally, it is interesting to decompose the dipole moment per unit into the charge and current components shown in the 3rd and 4th rows of Fig. 4. For the present model, the current contribution is the one that shows the strongest dependence on E and on $\tilde{n}$. It follows from Eq. 40 that the major part of the finite chain (hyper)polarizabilities arises from the terminations. Since the unit cells of the central region remain neutral, the variation in the charge contribution due to the field results solely from a redistribution of the charge within the individual unit cells. On the other hand, the variation in the current contribution comes

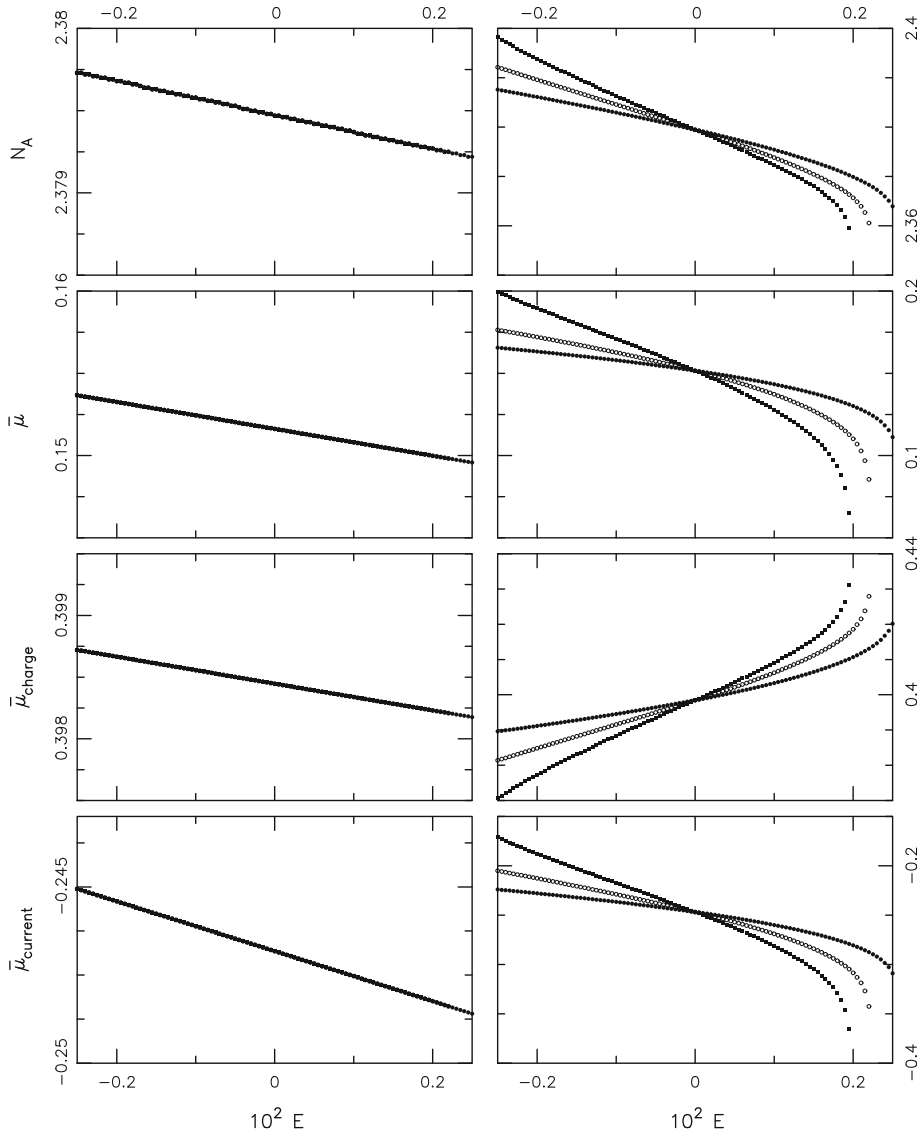

Fig. 4 Various properties of the infinite periodic chain as a function of the field, *E*. *Different symbols* mark results for different values of the missing integer, $\tilde{n}$. The *upper* panels show the Mulliken gross population on one of the two atoms of the unit cell. The *second* row shows the dipole moment per unit; it is split into a charge contribution term (*third* row) and a current contribution (*fourth* row). The *left hand* panels show the results without structure relaxation (i.e., for the optimized structure in the field-free case), whereas the results in the *right hand* column include structure relaxation. In order to make the comparison more clear, the results of the 2nd and 4th row have been modified by an appropriate integer times the field-free lattice constant. Notice the different scales for the ordinate

from a charge transfer from one end to the other, whose magnitude is independent of the size of the system.

5 Determination of piezoelectric and vibrational linear/non-linear optical properties from nuclear response

As implied in Sect. 4.3, the results shown in Figs. 3 and 4 can be used to determine piezoelectric coefficients and the contribution of nuclear relaxation to (hyper)polarizabilities. We shall here discuss these issues a little further.

5.1 Piezoelectricity

The results of Fig. 3 give information on the piezoelectric parameters of the system at hand. Piezoelectricity originates from a coupling between mechanical and electric properties. One may study different piezoelectric effects (see e.g., [24]) but here we will concentrate on the converse piezoelectric effect, i.e., the production of stress or strain when an electrostatic field is applied.

In our case, where the field as well as the chain are along the z direction, the corresponding converse piezoelectric coefficient d_{zz} is defined through

$$\frac{\Delta L}{L_0} = d_{zz}E. \tag{52}$$

Here, L_0 is the total zero-field length of the macroscopic sample and ΔL is its change in length due to the applied electrostatic field. We split the total length of the sample, L, into a sum of contributions from the three regions of Fig. 1a, b or c each with its own converse piezoelectric coefficient,

$$\begin{aligned} L &= L_0 + \Delta L \\ &= L_R + L_L + N_C \cdot a \\ &= L_{R0}(1 + d_{zzR}E) + L_{L0}(1 + d_{zzL}E) + N_C a_0(1 + d_{zzC}E). \end{aligned} \tag{53}$$

Here, d_{zzC} is the slope of a as a function of E for $E \rightarrow 0$. The results of Fig. 3 illustrate how this quantity can be extracted from nuclear response calculations.

Equation 53 can alternatively be written as

$$\begin{aligned} L = L_0(1 + d_{zzC}E) + L_{R0}(d_{zzR} - d_{zzC})E \\ + L_{L0}(d_{zzL} - d_{zzC})E. \end{aligned} \tag{54}$$

Thus, in order to determine experimentally the converse piezoelectric coefficient for the bulk region, one should study different samples that differ in length but have exactly the same terminations. Plotting L as a function of L_0 for a given field strength will result in a straight line whose slope is $1 + d_{zzC}\ E$. Our finding for the infinite, periodic system that a depends on the missing integer shows that, although this slope is a purely bulk property, it depends on the missing integer. That is to say, it depends on the charge accumulated at the surfaces. Changing the terminations will, in general, lead to a straight line with a different slope.

5.2 Vibrational linear and non-linear optical properties

In this sub-section, we explore the feasibility of calculating vibrational static (hyper)polarizabilities as well as dynamic non-linear optical properties by means of the finite field nuclear relaxation (FF-NR) procedure [25]. For static (hyper)polarizabilities, we begin with the usual expansion of the dipole moment per unit as a power series in the applied electrostatic field

$$\bar{\mu}(E) = \bar{\mu}_0 + \alpha E + \beta E^2 + \gamma E^3 + \cdots. \tag{55}$$

In Eq. 55 $\bar{\mu}_0$ corresponds to the permanent dipole moment per unit, α to the static polarizability per unit, and $\beta, \gamma, \cdots$ to the 1st, 2nd, $\cdots$ static hyperpolarizability per unit. These properties may be determined by calculating $\bar{\mu}(E)$ for several different values of E and subsequently fitting the results to a polynomial of varying length. Although more sophisticated procedures could be applied, the fitting in this initial exploratory study is done by means of least squares. In addition, we choose to use only those field values for which

$$|E| \leq \max|E|. \tag{56}$$

It is important to note that the geometry has not yet been specified. Two obvious possibilities are the field-free geometry in all cases or the fully relaxed geometry at each field. The former choice gives the static electronic (hyper)polarizabilities, whereas the difference between the two yields [25] the FF-NR approximation for the static vibrational (hyper)polarizabilities. This approximation accounts for the zeroth-order double harmonic (electric and mechanical) contributions plus the leading perturbation theory corrections [26].

The results of our fits are displayed in Fig. 5. Only one value of the missing integer is utilized, but that is sufficient for current purposes. The quantities of interest, as indicated above, are the differences between the values in the right hand panels (relaxed geometry) and those in the corresponding left hand panels (field-free geometry). In order to have a well-defined vibrational (hyper)polarizability, this difference must be constant (or nearly constant) over a range of maximum fields. The figure shows, as expected, that including fields that are too large (i.e., choosing too large a value for $\max|E|$), leads to unstable results. On the other hand, $\max|E|$ should also not be too small, especially if the second hyperpolarizability is desired. In most instances, it seems that our goal has been fairly well achieved. The worst case, perhaps, is the second hyperpolarizability of the relaxed structure. Even then, however, there is a reasonable range of maximum fields over which the third-order fit gives a nearly constant value. An improved result would most likely be obtained with the use of a different fitting procedure. However, that is beyond the scope of the present work.

Except for $\bar{\mu}_0$ the vibrational contribution to the property value is much larger in magnitude than the electronic contribution in the current model. This is a consequence of the fact that $\bar{\mu}$ depends much more strongly on E when the structure is relaxed as we have seen in Sect. 4.3 The fact that $\bar{\mu}_0$ is unchanged by nuclear relaxation is as it should be since the only vibrational contribution to the permanent dipole moment is due to zero-point motions. The latter is a separate, normally small, effect that is also not included in any of the FF-NR vibrational (hyper)polarizabilities.

The above treatment can be extended to obtain dynamic vibrational hyperpolarizabilities in the so-called infinite optical frequency approximation [25], which applies when the frequency of the incident light wave, ν, is such that the $\nu_{\text{vib}} \ll \nu$ for all fundamental vibrational frequencies, ν_{vib}. For this purpose, a 'pump' field is applied to define the structure of the system and, at this fixed structure, a separate set of 'probe' fields is utilized to obtain the electronic linear polarizability and first hyperpolarizability per unit from the expansion in Eq. 55. In Fig. 6, we show how these properties vary for a set of different structures generated by the 'pump' field given on the horizontal axis. These results were obtained with a maximum 'probe' field of magnitude 0.0025 and different power series fits. Again, the desired quantities are the differences between property values at the zero-field geometry (see relevant left hand panels of

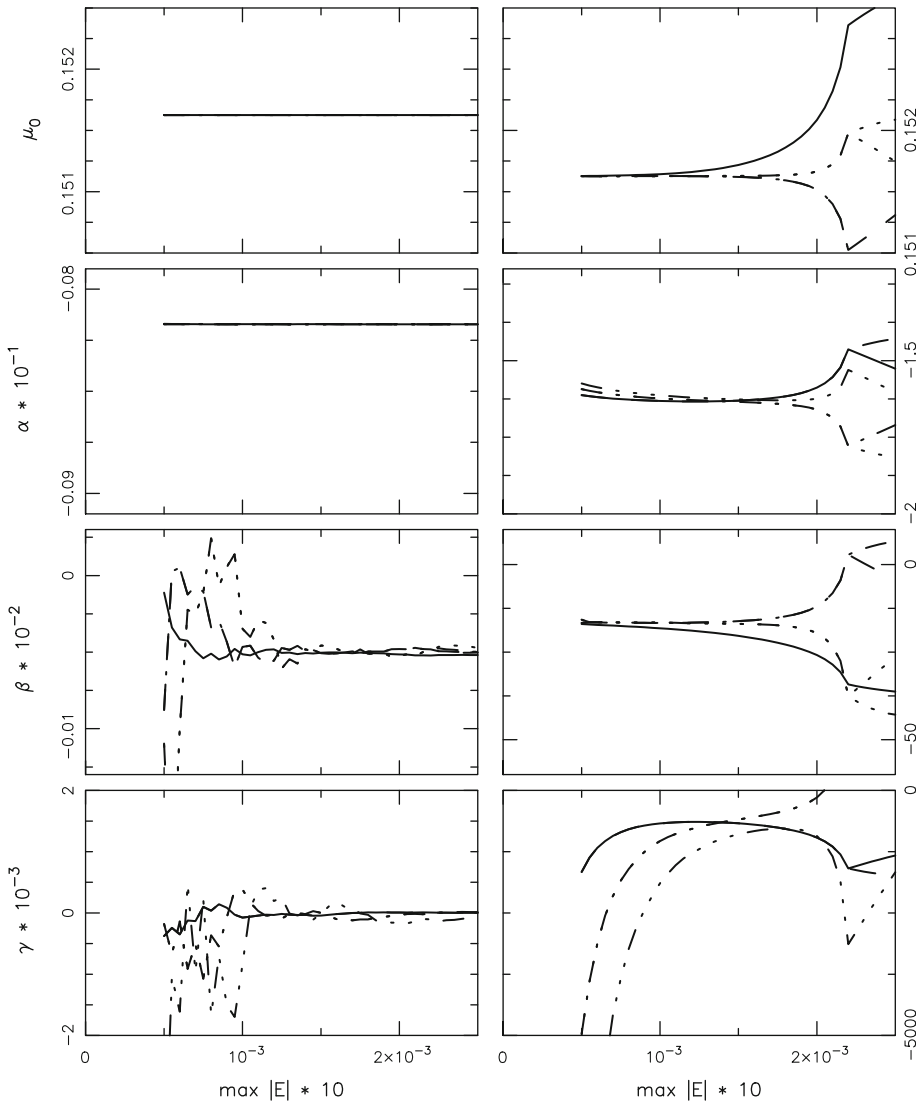

Fig. 5 The various coefficients in the expansion of Eq. 55 as a function of the maximum absolute value of the field used in the fit. The *solid*, *dashed*, *dash-dotted*, *dotted*, and *dash-dot-dot-dotted* curves represent fits with a 3rd, 4th, 5th, 6th, and 7th order polynomial, respectively, and the structure has been fixed at that of the field-free case in the *left* panels, whereas it was relaxed in the *right* panels

Fig. 5) and at the geometry defined by the 'pump' field. Expanding the difference in α as a function of 'pump' field (cf. Eq. 55) yields the vibrational dc-Pockels (dc-P) β as the linear term and the vibrational electro-optic Kerr effect (EOKE) γ as the quadratic term; the analogous expansion of β gives the vibrational contribution to dc-second harmonic generation (dc-SHG) as the linear term. The first-order and second-order (for α) approximations obtained by fitting the property data are also shown in Fig. 6. Although the fitting can be improved, one can judge from this figure the viability of the FF-NR method for determining the zero-field derivatives that yield the vibrational dc-P, EOKE, and dc-SHG non-linear optical properties.

As far as we know, there are no calculations in the literature for infinite periodic structures that utilize the methodology just presented and very few, by any means, for the vibrational properties (other than static polarizability) studied here. Considering the large magnitude that may often occur for the vibrational, as opposed to electronic, (hyper)polarizabilities this nuclear relaxation methodology deserves further exploration and application.

6 Discussion and conclusions

In this contribution, we have focused on an apparently trivial issue: how to calculate the dipole moment per unit for a regular quasilinear system that is so large that it is most conveniently treated as being infinite and periodic. Only during the past 1–2 decades have satisfactory approaches been suggested for calculating $\bar{\mu}_z$. Surprisingly, in the MTP approach, no mathematical derivation has previously been given although, as we show here, it is indeed possible to do so. From this derivation, one can understand the consequence of limiting the number of k points in any practical calculation. Moreover, it leads

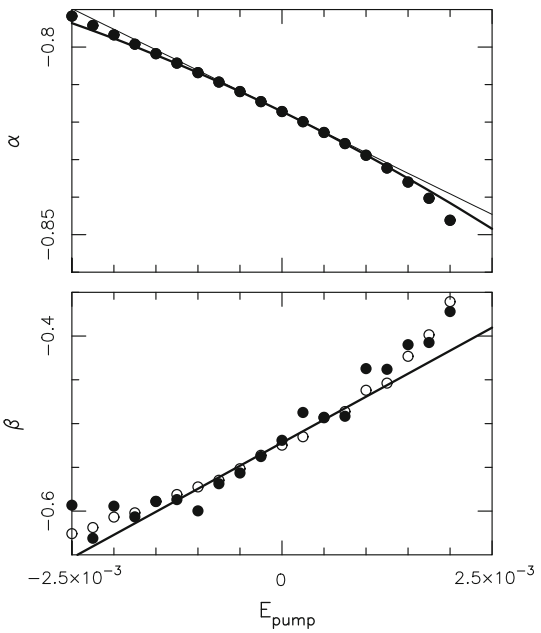

Fig. 6 Variation in α and β at the geometry defined by the pump field specified on the horizontal axis. The property values were determined by fitting the dipole moment to a third-order (*open circles*) and fifth-order (*filled circles*) polynomial in a set of probe fields with maximum magnitude of 0.0025. The *thick solid curves* show a second-order (*upper* panel) and first-order (*lower* panel) fit to the results around vanishing pump field. In the *upper* panel, the second-order term has been omitted for the results of the *thin solid curve*

directly to a treatment of electron correlation from a multi-determinant wavefunction point of view, which has not heretofore been available. We also suggest that electron correlation can most readily be incorporated within the VPA by combining two procedures that are already available, namely time-dependent MP2 and 'local' MP2 for periodic systems.

It is interesting that, upon substitution at the terminations, $\bar{\mu}_z$ for the large, but finite, system can vary by only an integer times the lattice constant. There is a similar contribution to the calculated dipole moment of an infinite periodic system, which arises because of an indeterminacy in a phase angle (known as the branch-dependence). We have confirmed in model calculations that the two cases are completely equivalent. This implies that, independent of the size of the large finite system, the terminations make a finite contribution to a number of experimental observables. They also affect the value of the field-dependent bulk lattice constant which, in turn, will induce changes in other properties. Through Zener tunneling, this effect will also depend on the size of the finite system even if it is so large that it can be considered above the thermodynamic limit. Zener tunneling takes place when the field strength is so large that it is energetically advantageous for electron(s) to be transferred from one end of the system to the other. For systems of different lengths but exposed to the same field strength, Zener tunneling may occur for longer chains but not for shorter ones. This transfer of charge will cause the 'missing integer' to change in value (even though self-consistent field calculations can become problematic [27].

It is non-trivial to set up and solve the VPA equation [8, 9] for the field-dependent geometrical structure of the infinite periodic system even in the independent particle case. In recent years, however, we have been able to develop an efficient and accurate method for this purpose [11, 12, 14, 16]. Using that method for model systems, we have found structural responses and thereby obtained the converse piezoelectric coefficient. This bulk property was shown to depend upon the missing integer and an experimental procedure was outlined for determining, in principle, the effect of the terminations.

We have also demonstrated how the structural response, in conjunction with the FF-NR procedure, can be utilized to obtain static vibrational (hyper)polarizabilities as well as several dynamic vibrational non-linear optical properties. The potential significance of these properties has been indicated and, in many instances, this is the first time a practical computational method has been demonstrated for a periodic system.

In principle, it is possible to generalize the treatment presented here to higher dimensions, although additional complications may occur. Most notably, surface reconstructions can lead to surface unit cells that are larger than those in the bulk. As a result, there may be additional contributions to $\bar{\mu}$ that cannot be treated directly within a periodic system approach without having to use a larger unit cell. This situation is, however, beyond the scope of the present contribution.

Finally, for the sake of completeness, we add that the approach presented here, and applied for a simple model, is currently being implemented in ab initio programs. A preliminary discussion of this work has been presented earlier [16], and in the future, we hope to present ab initio results on the responses of real systems to electrostatic fields.

Acknowledgments One of the authors (MS) is very grateful to the International Center for Materials Research, University of California, Santa Barbara, for generous hospitality.

References

1. Blount EI (1962) Solid State Phys 13:305
2. King-Smith RD, Vanderbilt D (1993) Phys Rev B 47:1651
3. Vanderbilt D, King-Smith RD (1993) Phys Rev B 48:4442
4. Resta R (1994) Rev Mod Phys 66:899
5. Resta R (1999) Int J Quant Chem 75:599
6. Resta R (2010) J Phys Cond Matter 22:123201
7. Otto P (1992) Phys Rev B 45:10876

8. Kirtman B, Gu FL, Bishop DM (2000) J Chem Phys 113:1294
9. Bishop DM, Gu FL, Kirtman B (2001) J Chem Phys 114:7633
10. Springborg M, Kirtman B, Dong Y (2004) Chem Phys Lett 396:404
11. Springborg M, Kirtman B (2007) J Chem Phys 126:104107
12. Springborg M, Kirtman B (2008) Phys Rev B 77:045102. Erratum: Springborg M, Kirtman B (2008) Phys Rev B 77:209901
13. Springborg M, Kirtman B (2008) Chem Phys Lett 454:105
14. Springborg M, Kirtman B (2009) Can J Chem 87:984
15. Springborg M, Tevekeliyska V, Kirtman B (2010) Phys Rev B 82:165442
16. Springborg M, Tevekeliyska V, Kirtman B, Champagne B, Dong Y (2010) Z Phys Chem 224:617
17. Nunes RW, Gonze X (2001) Phys Rev B 63:155107
18. Kudin KN, Car R, Resta R (2007) J Chem Phys 127:194902
19. Ashcroft NW, Mermin ND (1976) Solid state physics. Saunders College Publishing, Orlando
20. Martin RM (2004) Electronic structure. Cambridge University Press, Cambridge
21. Tagantsev AK (1991) Phase Transitions 35:119
22. Hattig C, Hess BA (1995) Chem Phys Lett 233:359
23. Pisani C, Busso M, Capecchi G, Casassa S, Dovesi R, Maschio L, Zicovich-Wilson C, Schütz M (2005) J Chem Phys 122:094113
24. Boonchun A, Lambrecht WRL (2010) Phys Rev B 81:235214
25. Bishop DM, Hassan M, Kirtman B (1995) J Chem Phys 103:4157
26. Bishop DM, Kirtman B (1992) J Chem Phys 97:5255
27. Springborg M Unpublished results